Scientific Research Publishing

Journal of Materials Science and Chemical Engineering, 2026, 14(11), 42-58
https://www.scirp.org/journal/msce
ISSN Online: 2327-6053
ISSN Print: 2327-6045

# Effective Interfacial Layer Formation with an Optimized LiDFOB Additive and Its Analysis by Electrochemical Impedance Spectroscopy (EIS) in Lithium-Ion Batteries

**Seggem Prabhakar*, Kirankumar Rajendranath, Satyanarayana Maddukuri, Vasudeva Rao Pasala, Ebenezer Duggapogu, Aditya Ranjan Ray**

Amararaja Advanced Cell Technologies, Gachibowli, Hyderabad
Email: *sp7@amararaja.com

**How to cite this paper:** Prabhakar, S., Rajendranath, K., Maddukuri, S., Pasala, V.R., Duggapogu, E. and Ray, A.R. (2026) Effective Interfacial Layer Formation with an Optimized LiDFOB Additive and Its Analysis by Electrochemical Impedance Spectroscopy (EIS) in Lithium-Ion Batteries. *Journal of Materials Science and Chemical Engineering*, **14**, 42-58.
https://doi.org/10.4236/msce.2026.1411003

**Received:** July 21, 2026
**Accepted:** November 13, 2026
**Published:** November 16, 2026

Copyright © 2026 by author(s) and Scientific Research Publishing Inc.
This work is licensed under the Creative Commons Attribution International License (CC BY 4.0).
http://creativecommons.org/licenses/by/4.0/

Open Access

## Abstract

Lithium difluoro(oxalate)borate (LiDFOB) has emerged as an applicable electrolyte additive for enhancing the stability and ionic conductivity of both the solid electrolyte interphase (SEI) and the cathode electrolyte interphase (CEI) in conventional carbonate-based lithium-ion batteries. This study illustrates that the addition of 1 wt% LiDFOB to organic solvent-based electrolytes markedly enhances the cycling performance of NMC bimodal/Li cells, attaining over 81% capacity retention in contrast to merely 65% in baseline electrolytes. Electrochemical impedance spectroscopy (EIS) and cyclic voltammetry (CV) validate the establishment of a robust and low-resistance electrode/electrolyte contact on the surfaces of both the anode and cathode. Additionally, EIS and scanning electron microscopy (SEM) investigations of NMC bimodal–graphite complete cells indicate that the CEI produced from LiDFOB reduces internal resistance. Inductively coupled plasma atomic emission spectrometry (ICP-AES) offers further proof that LiDFOB efficiently inhibits transition metal dissolution from the cathode during high-voltage operation. These findings underscore LiDFOB as a very efficacious addition for enhancing the electrochemical stability and longevity of high-energy lithium-ion batteries, facilitating its practical application in next-generation energy storage systems.

## Keywords

LIB, Electrolyte, SEI Layer, Impedance

## 1. Introduction

The escalating accumulation of greenhouse gases (GHGs), notably $CO_2$ and $N_2O$, predominantly due to persistent dependence on fossil fuels, has precipitated substantial environmental alterations, including global warming and climate change. A move to sustainable and cleaner energy alternatives is urgently required to mitigate these implications. The adoption of electric vehicles (EVs) represents a promising answer, providing a viable alternative to fossil fuel-powered transportation. The increasing demand for electric vehicles, coupled with their incorporation into consumer electronics and industrial systems, has accelerated the swift advancement and implementation of rechargeable Li-ion batteries (LIB), recognized for their high energy density and extended cycle life. Due to the very high theoretical specific capacity of Li metal (*i.e.*, 3.86 $Ah \cdot g^{-1}$) and its low reduction potential (−3.04 V vs. SHE), Li metal has received much attention as a prospective anode material for advanced lithium-ion batteries with high energy density [1] [2]. To maximize the advantages of Li metal and address the escalating performance requirements of contemporary energy storage systems, researchers are concentrating on the development of high-voltage, high-capacity cathode materials that may function synergistically with lithium-based anodes. Collectively, these initiatives seek to produce batteries with enhanced energy density and efficiency, facilitating the global transition to sustainable energy solutions [3].

Electrolytes have a very important part to play in LIB systems when it comes to electrochemical performance. Commonly used electrolytes involve lithium hexafluoro phosphate ($LiPF_6$) in a solution with a combination of two or more organic solvents like ethylene carbonate (EC), propylene carbonate (PC), ethyl methyl carbonate (EMC), dimethyl carbonate (DMC), and diethyl carbonate (DEC). These solvents are selected for their ability to dissolve lithium salts effectively and provide wide electrochemical stability windows. However, during the initial activation process of LIBs, these electrolyte components are not entirely stable and tend to undergo sacrificial decomposition at the electrode surfaces. The above process leads to the development of the passivation layer, specifically the solid electrolyte interface (SEI) at the anode side and the cathode electrolyte interface (CEI) at the cathode side, which is crucial for the stabilization of the electrode-electrolyte interfaces [4].

The creation of specialized electrolytes with functional additives is becoming ever more popular as an essential strategy for improving LIB's energy density, cycle life, and safety performance. This is primarily attributable to the roles that the corresponding additives played: 1) enhance the physical properties of the electrolyte such as viscosity, transfer number, ionic conductivity and wettability 2) stabilizing the SEI film to reduces the redox reactions 3) increases the fire-retardant of the carbonate-based electrolytes 4) improving thermal stability of $LiPF_6$ with in the organic solvents 5) giving the overcharge protection [5]. The formation of Li dendrites brought on by the uneven deposition of lithium is a significant safety concern. Lithium metal and the electrolyte undergo a harmful side reaction that

leads to the production of lithium dendrites, a short cycle life, and safety concerns because of the instability of the SEI of metallic lithium [6]. In the last five years, most researchers have concentrated on layered nickel-rich metal oxides characterized by the general formula Li (NixMnyCoz) $O_2$ (where $x \geq 0.6$ and $x + y + z = 1$). These materials have garnered interest owing to their superior capacity and reduced cost relative to $LiCoO_2$, rendering them particularly appealing as cathode materials for high-energy-density lithium-ion batteries [7]-[9]. However, a significant problem is emerging that prevents the widespread use of nickel-rich oxides by causing electrolyte breakdown on the positive electrode surface, which is catalyzed by the highly oxidative $Ni^{3+}/Ni^{4+}$ [10] [11]. The formulation of innovative additions to improve the stability and efficacy of electrolytes has been the subject of an increasing number of studies [12]. In order to provide SEI film with strong thermal stability, additives such as vinylene carbonate (VC) are reduced before organic carbonates during the first cycle. Nevertheless, the thermal breakdown of lithium hexafluoro phosphate salt ($LIPF_6$) cannot be prevented by VC [13] [14].

More weight percentage of VC-based electrolytes shows higher charge transfer resistance at anode surface area and in most of cases 1 - 2 wt% VC is sufficient [15]. VC-based electrolytes aids to reduce the gas evolution in EC related electrolytes and change the primary gas produced from ethylene to $CO_2$ [16]. The optimized electrolyte additive can comprise both inorganic & organic functional groups for example fluoroethylene carbonate (FEC) [17], tris (trimethylsilyl) phosphite (TMSP) [18], lithium bis (oxalato)borate [19] [20], LiDFOB [21].

Currently utilized in commercial LIB, the $LiPF_6$ salt reacts more strongly to water traces in the electrolytes [22], and it will create HF gas that corrodes the electrode surface, particularly at high temperatures. The incorporation of mixed lithium salts or the introduction of electrolyte additives have been widely considered as viable solutions to this problem [23]-[25]. LiDFOB is used to provide a stable SEI coating that protects the electrode from erosion by the electrolyte solvent in order to effectively improve the electrochemical performance of graphite [26]. LiDFOB additive has shown enhanced electrochemical performance on cathode materials, for example, $LiFePO_4$ [27], $LiMn_2O_4$, [28] and $LiNi_{1/3}Co_{1/3}Mn_{1/3}O_2$ [29] and mixed with ionic liquid electrolyte as N-butyl-methylpiperidi-niumbis (trifluoromethylsulfonyl) imide (PP14TFSI) and tetra-methylenesulfone (TMS) [30]. LiDFOB enhances graphite electrochemical performance by forming a stable SEI that protects the electrode from electrolyte degradation [26] and a CEI on high-voltage cathodes at elevated temperatures [31]-[33]. Gao *et al.* reports that the LiDFOB additive in a carbonate electrolyte will give good performance of NMC//Li half-cells chemistry [31] and LiFSI electrolytes in the LiDFOB additive as shown outstanding as a non-corrosive protecting film for the Al current collector used in $LiCoO_2$||graphite cell, in this Al-F, $Al_2O_3$ and B-O passivation layer will be formed [34]. In adding of the LiDFOB additive to the carbonate electrolyte enhanced electrochemical performance in $Li_{1.17}Ni_{0.17}Mn_{0.5}Co_{0.17}O_2$||graphite cells [35].

In this study, we examine how improved electrolyte additives affect the electro-

chemical performance of Li/NMCbimodal ($LiNi_{0.85}Mn_{0.05}Co_{0.1}O_2$) cells. Three additive formulations were investigated: base electrolyte with 2 weight % VC, base electrolyte with 2 weight % VC and 1 weight % LiDFOB, and base electrolyte with 2 weight% VC and 2 weight % LiDFOB. The basic electrolyte consists of 1 M $LiPF_4$ dissolved in EC/DEC/EMC (1:1:1, weight percent). Within an electrochemical range of 2.8 - 4.3 V vs. Li/Li, these formulations were assessed in Li/NMC bimodal cells under varied C-rates and cycling conditions. An EIS analysis was carried out at various cycling phases to track the evolution of interfacial resistance.

The electrolyte with 1 weight % LiDFOB showed the best rate capability and cycle stability among the studied formulations. The cycled NMCbimodal cathode developed a strong, LiF-rich, boron containing CEI layer, according to post-mortem studies employing FE-SEM, EDX, and TEM. This modified electrolyte successfully reduced transition metal dissolution and prevented the development of a cation-disordered layer on the exposed cathode surface in graphite/NMC bimodal complete cells, improving structural and electrochemical stability.

The current work reveals 1 wt% LiDFOB as an optimized electrolyte additive to improve the electrochemical behavior and interfacial properties of NMC bimodal-based lithium-ion cells. In particular, it is shown that LiDFOB facilitates the development of robust and ionically conductive SEI/CEI film, which in turn results in low interfacial resistance and compatibility between electrodes and electrolytes. The optimized electrolyte shows a very high specific capacity of around 190 $mAh{\cdot}g^{-1}$, while retaining ~85% of the capacity at 90 cycles, showing great superiority to VC-based and pristine electrolytes. In addition, the analysis from EIS, SEM, and ICP-MS reveals low internal resistance and limited transition metal dissolution, especially manganese.

## 2. Experimental

### 2.1. Preparation of Electrodes

The baseline electrolyte was prepared with 1 M $LiPF_6$ in ethylene carbonate/di ethyl carbonate/ethyl methyl carbonate (EC/DMC/EMC as 1:1:1 wt% ratio), obtained from Kishida Co., Ltd. Additives such as VC and LiDFOB were from sigma Aldrich different wt% of the additives were mixed with the baseline electrolyte and stirred till completely mixed. These were all carried out in a high-purity Argon-filled glovebox (Braun, Frankfurt, Germany) with less than 0.5 ppm of $O_2$ and moisture. The NMC bimodel electrodes were prepared by casting the mixing slurry, NMCbimodel commercial grade, C65T & KS6L grades from sigma Aldrich and polyvinylidene fluoride from Solvey Co., Ltd. (96:0.7:0.8:2.5 wt% ratio) dispersed in N-methyl-2-pyrrolidineone, (NMP, sigma Aldrich) coated on Al foil (thickness 15 μm) and pre drying in an infrared oven. The active material in each electrode was ~21 $mg{\cdot}cm^{-2}$. The prepared electrode was dried in a vacuum oven at 120˚C for 12 h. Coin cell was assembled using CR2032 stainless steel coin cell case in which NMC bimodel as the positive electrode, Li metal as negative electrode, and the base electrolyte and additive combined electrolyte were tested re-

spectively. Double side ceramic coated 16 μm separators from commercial grade were used In anode active material is 95%, C65T is 1% and PVDF is 4%.

### 2.2. Electrochemical Measurement

The assembled coin cell (NMC bimodel/Li metal) was aged for 24 h before testing. The cells were tested using (Neware instrument) for charge/discharge at different C-rates at ambient temperature. The cells went through three formation cycles at a rate of 0.1 C in the voltage range of 2.8 to 4.3 volts. This helped create the CEI. The 1 C rate is the same as 180 $mAh \cdot g^{-1}$. After that, the long-term performance of the NMC bimodal/graphite cells was tested over 60 cycles. They charged at 0.5 C and discharged at 0.33 C. EIS was done with a BioLogic electrochemical workstation when the cells were fully charged at 4.3 volts. The impedance data was collected three times for each cell. The AC signal was ±10 mV. The frequency range was from 10 kHz, to 10 mHz. The voltammetric scan speed was kept at 0.1 $mV \cdot s^{-1}$.

### 2.3. Characterizations

Each coin cell (NMCbimodel/Li metal) prepared with different additive combinations after 200 cycles were disassembled inside glovebox. Following cycling, the electrodes were dried in an oven after soaking them in DMC to eliminate any remaining Li salts and electrolyte. A FE-SEM (S-4800, Hitachi) was used to analyze the surface morphology of the cycled electrodes. The LiDFOB additive's ability to inhibit transition-metal dissolution was assessed using ICP-AES (Bruker Scientific). Specifically, ICP-AES was used to measure the Ni content deposited on the cycled lithium anode in order to evaluate transition-metal migration and deposition during cycling.

## 3. Results and Discussion

### 3.1. Half-Cell Charge-Discharge Performance

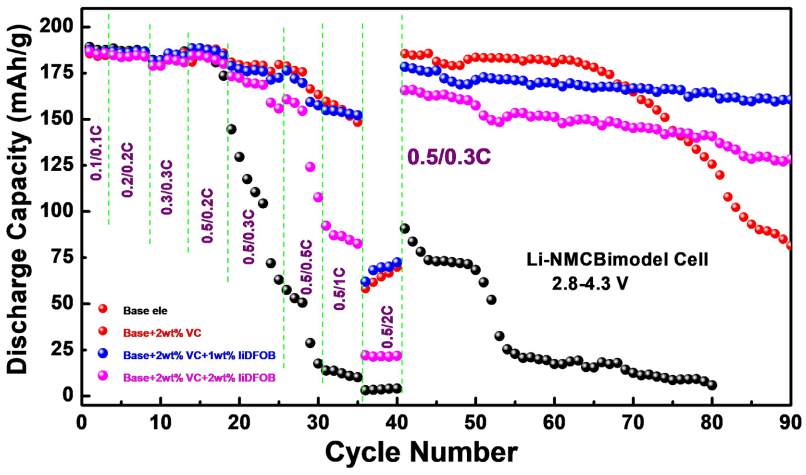



Figure 1. Representative the NMCbimodel/Li half-cell at different C-rate and long cycle life (0.5 C/0.33C rate) performance with different electrolyte compositions.

The galvanic charge-discharge performance on NMCbimodel/Li cells electrochemical potential window range as 2.8 - 4.3 V under different C-rates and reveals that electrolytes containing base, VC, 1 wt% LiDFOB and 2 wt% LiDFOB composition electrolytes. Figure 1 shows the discharge capacity of NMCbimodel/Li cells cycled in the range of 2.8 - 4.3 V under different rates and reveals that electrolytes containing 1 wt% LiDFOB composition exhibit the best rate capabilities compare to another base, VC and 2 wt% LiDFOB electrolyte compositions. The 1 wt% LiDFOB shown higher retention at 0.5 C/.33C C-rate compared remaining electrolyte compositions. Furthermore, the capacity of baseline NMC bimodel/Li cells at 0.5 C/.33C could not be recovered after cycling at 2 C rate performance. The continue charge-discharge 0.5 C/0.33C condition the base + 2 wt% VC electrolyte gives small cycle compared to base + 2 wt% VC + 1 wt% LiDFOB electrolyte. These findings show that faster $Li^+$ transit on the Ni-rich positive electrode was made possible by CEI produced in the presence of the LiDFOB addition. Given that the LiDFOB is intended to be decreased on the Li negative electrode before the carbonate solvents form the SEI layer on the Li negative electrode surface, this could enhance the NMCbimodel/Li cells' electrochemical performance.

### 3.2. Electrochemical Impedance Spectroscopy (EIS) Studies

EIS tests applies on different electrolyte compositions like that base, VC, 1 wt% LiDFOB and 2 wt% LiDFOB are used for NMCbimodel/Li cell with at 10 KHz to 10 mHz with 10 mV amplitude. The EIS spectra are shown in Figures 2(a)-(d), each of which has two semicircular arcs followed by an inclined straight line. Li ion transport across the interfacial layer is influenced by the resistance of the surface film generated on the electrode, which is responsible for the first semicircle in the high-frequency region. The charge-transfer resistance (Rct) at the electrode–electrolyte interface is represented by the second semicircle in the medium-frequency region. The Warburg impedance, which is linked to the diffusion of Li+ ions inside the bulk material of the electrode, is shown by the inclined line in the low-frequency zone. These impedance characteristics shed light on the electrode system's interfacial characteristics and lithium-ion transport kinetics [36] [37]. The impedance values are shown in Table 1. EIS results reveal that these 1 wt% LiDFOB composition electrolytes show lesser impedance value at all stages compared to other composition electrolytes due to the formation of good contact CEI on cathode surface area [38].

Table 1. Representative Nyquist tabulation studied on the NMC bimodel/Li cell with various electrolytes at different stages completed cycles.

| Electrolyte compositions | After 3 cycles | After 40 cycles | After 60 cycles | After 90 cycles |
|---|---|---|---|---|
| Base | 26 | 93 | 147 | |
| Base + VC | 71 | 41 | 66 | 121 |
| 1 wt% LiDFOB | 31 | 39 | 65 | 75 |
| 2 wt% LiDFOB | 40 | 50 | 56 | 135 |

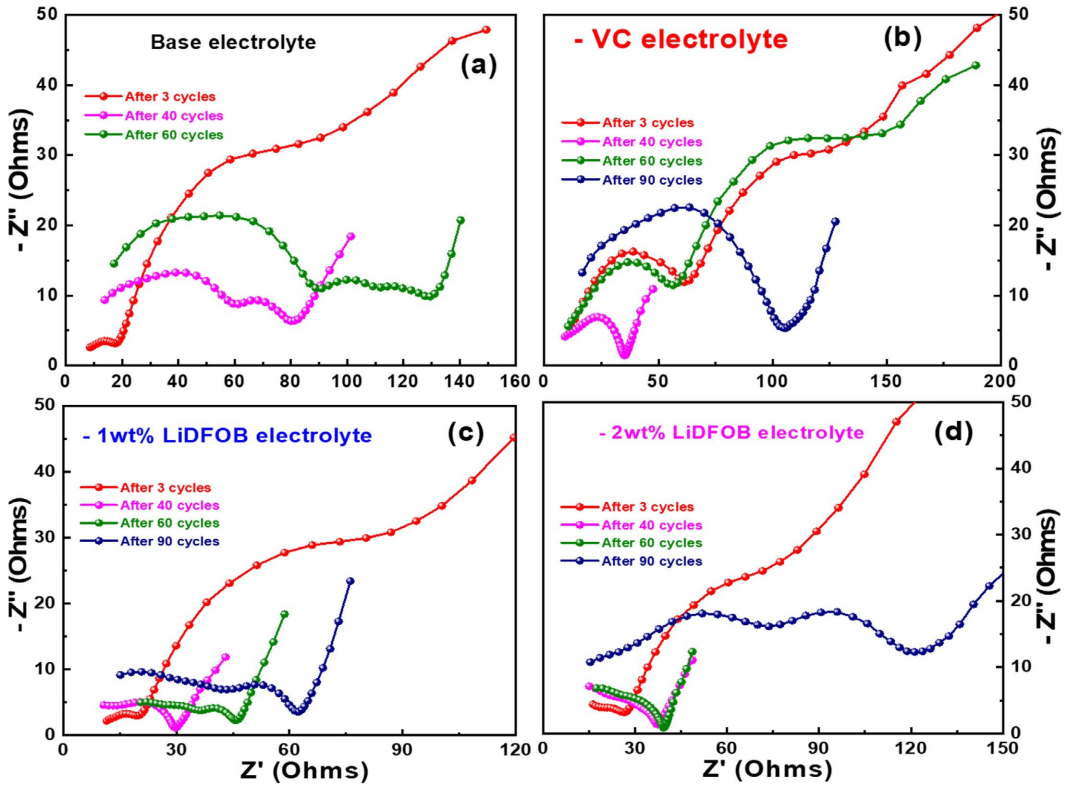



**Figure 2.** Representative the Nyquist plots studied on the NMC bimodel/Li cell with various electrolytes at different stages completed cycles.

### 3.3. Determination of Elemental Composition

The ICP-AES results from the lithium electrodes that were cycled and then taken from NMC bimodel||Li cells were studied so that we could see how the base electrolyte, VC and electrolytes with 1 LiDFOB or 2 wt% LiDFOB changed the amount of transition-metal deposition. In Table 2 we can see that the lithium electrode that was cycled in the electrolyte with 1 wt% LiDFOB had amounts of Mn, Ni and Co than the electrodes that were cycled in the base electrolyte or, in the electrolyte with 2 wt% VC. This means that adding LiDFOB really stops transition-metal from leaving the cathode and from settling on the lithium anode. Because LiDFOB breaks down first it can help make a CEI layer, which stops the electrolyte from breaking down and stops transition metals from moving around [39]. These results are in line with the process described by Amine *et al.* [40], who said that the bis(oxalato)borate ($BOB^{-}$) anion in lithium bis (oxalato) borate (LiBOB) can interact with dissolved $Mn^{2+}$ species and encourage the creation of a passivating layer on the cathode surface. Because LiBOB and lithium difluoro (oxalato)borate (LiDFOB) share structural similarities, a comparable interaction involving LiDFOB's oxalato-containing anion may help to stabilize the electrode-electrolyte interface and limit $Mn^{2+}$ dissolution. As a result, the decreased transition-metal deposition seen with 1 weight percent LiDFOB suggests that it may enhance long-term cycling performance and interfacial stability.

**Table 2.** Analysis of electrodes after electrochemical performance.

| Elements | Base electrolyte | Base + 2 wt% VC electrolyte | Base + 2 wt% VC + 1 wt% LiDFOB |
|---|---|---|---|
| Manganese (ppm) | 0.075 | 0.032 | 0.025 |
| Nickel (Ni) (ppm) | 0.591 | 0.21 | 0.192 |
| Cobalt (Co) (ppm) | 0.043 | 0.016 | 0.015 |

### 3.4. Morphological Examination of Electrodes

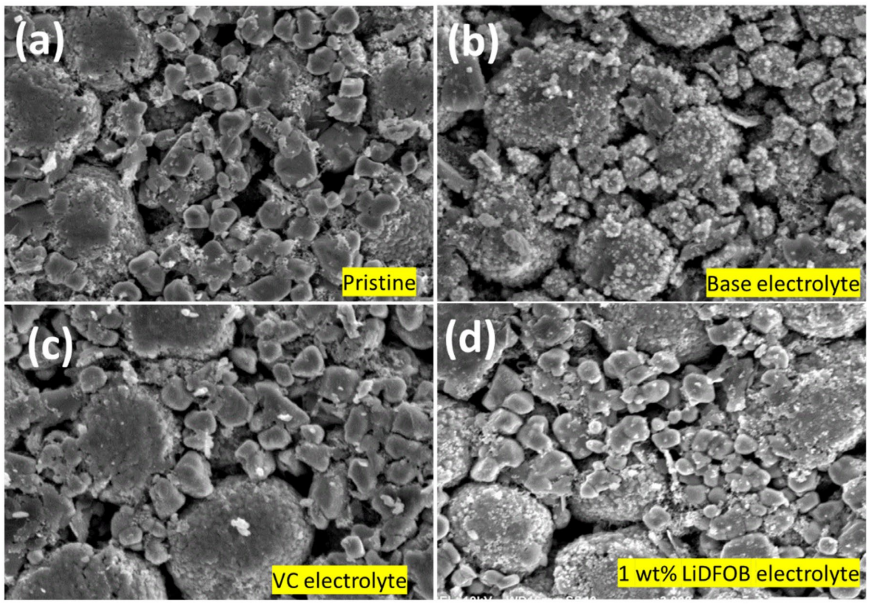



**Figure 3.** Representative the images of the (a) pristine and cycled graphite electrodes (b) base electrolyte (c) VC electrolyte (d) 1 wt% LiDFOB electrolyte from NMCbimodel/Li half-cell at room temperature.

Scanning electron microscopy (SEM) was used to analyze the surface morphology of the pristine and cycled NMC bimodel cathodes. The pristine electrode had a rather smooth and uniform surface, as seen in **Figures 3(a)-(d)**, but after 90 charge-discharge cycles, significant morphological changes were seen. The NMC particles showed significant surface breaking and deterioration in the baseline electrolyte, along with increased electrode surface roughness (**Figure 3(b)**). These alterations might be explained by ongoing electrolyte breakdown during cycling and parasitic interfacial interactions. On the contrary, the NMC particles cycled through the electrolyte with 1 wt% LiDFOB largely preserved their original morphology, which suggests that structural and interfacial stability has improved (**Figure 3(d)**). Furthermore, surface structures of the particles showed signs of having a different interface layer, which means that it leads to better and more effective CEI formation [41]. With respect to the reference electrolyte that previously led to uneven deposits, the electrolyte containing 1 wt% LiDFOB was shown to tend to create a more homogeneous electrode-electrolyte interface. Thus, it is

implied that preferential decomposition of LiDFOB leads to CEI formation that protects NMC bimodal cathode, which reduces parasitic electrolyte decompositions and improve interface stability during repeated cycling.

### 3.5. Cyclic Voltammetry Technique

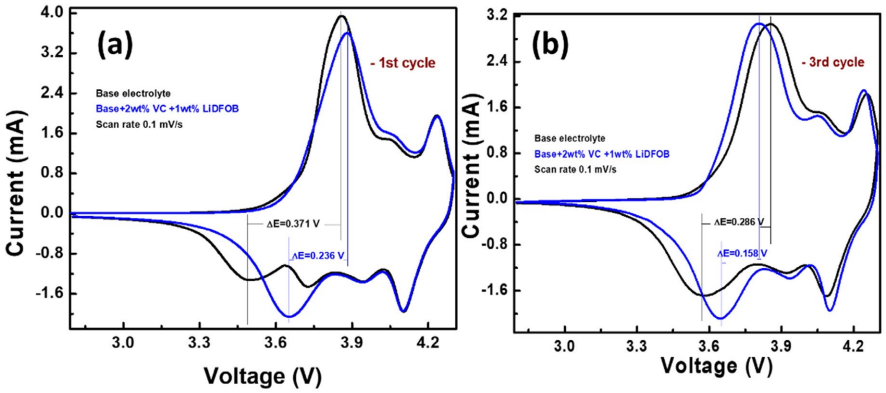



**Figure 4.** Representative the first three cycles cyclic voltammetry test conducted on NMCbimodel/Li cell (a) base electrolyte (b) 1 wt% LiDFOB electrolyte.

Cyclic voltammetry (CV) method mainly studies the kinetic mechanism of Li+ ions intercalation/de-intercalation in rechargeableLIB. The CV peaks of NMC bimodel/Li with applied potential from 2.8 - 4.3 V at the scan rate of 0.1 mV/s. **Figure 4(a)**, **Figure 4(b)** CV describes the three redox peaks observed which corresponded to the phase transition of H1 (hexagonal) → M (monoclinic), M (monoclinic) → H2 (hexagonal), and H2 (hexagonal) → H3 (hexagonal) [42]. **Figure 4(a)** shows redox peaks of NMCbimodel/Li cell at 3.949/3.672 V and 3.938/3.618 V corresponding to the first and third cycle, respectively, which indicates the phase transition of H1 → M. By adding 1 wt% LiDFOB in the electrolyte, the potential difference between the redox peaks at first and third cycle changed from 0.236 to 0.158 V, indicating the high stability of the phase structure. However, for the CV curves of NMC bimodel/Li cells with blank electrolyte, the difference between the redox peaks was changed from 0.371 to 0.286 V (**Figure 4(b)**), demonstrating that the 1 wt% LiDFOB is effective formation of CEI film formation cathode surface and it will to suppress the phase transformation during electrochemical process, which is helpful for improve the life cycle performance of Li/NMCbimodel cells.

### 3.6. Full-Cell Charge-Discharge Performance

To study the impact of an additive on electrochemical performance and stability, electrochemical cycling of NMC bimodal/graphite full cells using a regular electrolyte and a LiDFOB-containing electrolyte was conducted. The results presented in **Figure 5(b)** indicate that the cell with 1 wt% of LiDFOB exhibits better cycling performance compared to base electrolyte **Figure 5(a)** in the voltage range of 2.8 - 4.2 V. The initial discharge capacity went up from 49.6 $mAh{\cdot}g^{-1}$ for the cell with a regular electrolyte to 82.2 $mAh{\cdot}g^{-1}$ for the cell containing 1 wt% of LiDFOB. It

is seen that after 60 cycles the discharge capacity of the cell with a regular electrolyte and the cell with 1 wt% of LiDFOB is about 60 and 120 mAh·g$^{-1}$, respectively. The capacity retention in case of the cell with LiDFOB reached 81% in comparison with 50% for the cell with a regular electrolyte. Direct interactions between the electrode surface and dissolved transition-metal species can be restricted by the SEI that forms on the graphite anode. Nevertheless, interfacial deterioration and capacity fading may still be caused by transition metal deposition on graphite. Therefore, the development of more stable electrode-electrolyte interphases and the inhibition of transition-metal dissolution and migration may be linked to the enhanced cycle stability shown with LiDFOB. Figure 5(c) and Figure 5(d) depict the cycling test results conducted at a charge rate of 0.5 C and a discharge rate of 0.3 C. The starting discharge performance of the cell using 1 wt% LiDFOB was around 170 mAh·g$^{-1}$, while the conventional electrolyte cell showed 140 mAh·g$^{-1}$ performance. The LiDFOB cell attained over 80% retention while the conventional cell had about 60% retention, implying that the addition of LiDFOB indeed increased the retention performance. The faster fading of the conventional electrolyte may be partly due to the dissolution of transition metals from the cathode, which migrate to the anode and impact stability and performance negatively.

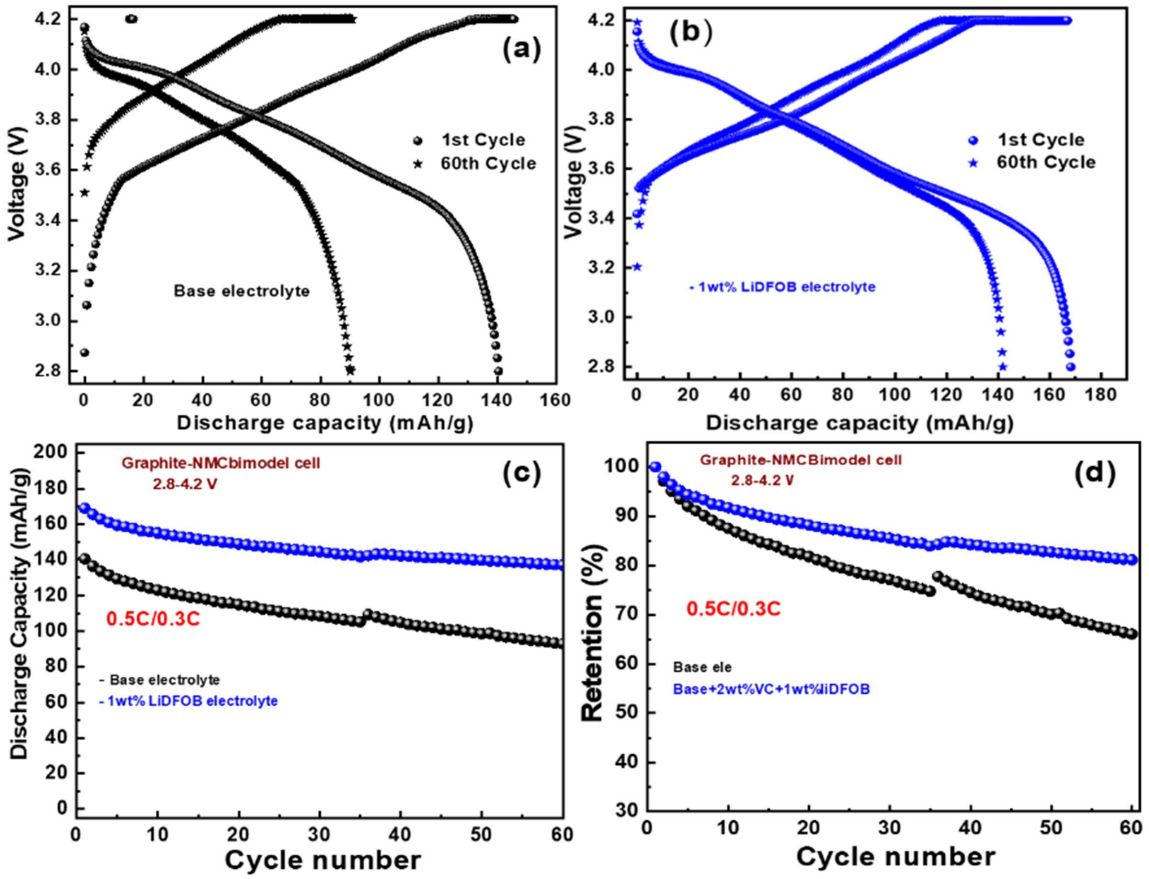



Figure 5. Representative the charge-discharge capacity performance on the (a) without and with (b) 1 wt% LiDFOB additive at a charge cutoff voltage of 2.8 - 4.2 V and (c) cycle life (d) retention NMCbimodel/graphite full cell.

### 3.7. Electrochemical Impedance Spectroscopy (EIS) Technic on Graphite-NMC Bimodel Cell

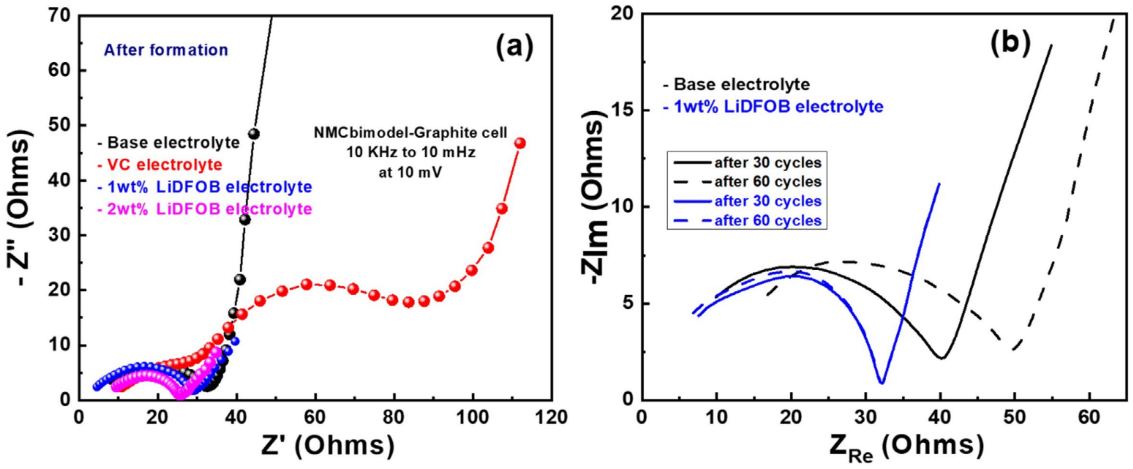



**Figure 6.** Representative the Nyquist plots studied on the NMC bimodel/Graphite cell with various electrolytes at different stages. (a) After formation (b) After 30$^{th}$ & 60$^{th}$ cycles completed

The utilization of EIS was made to determine how the incorporated electrolyte additives affect the electrochemical performance of the NMC bimodal versus graphite cells. The results show the Nyquist plots taken at the charging potential of 4.2 V after the formation cycles are displayed in **Figure 6**. Semicircular shapes in the high-to medium-frequency range denote the interfacial film resistance and charge-transfer resistance ($R_{ct}$), while the inclined line in the low-frequency region demonstrates the Warburg impedance indicating $Li^+$ diffusion through the active material. The studied electrolyte formulations were used in the first charge-discharge experiment where cells comprising of the standard electrolyte with the additions of 2 wt% VC and 1 wt% LiDFOB were found to show the lowest $R_s$ values of only 67.4 ohms in comparison with the other formulations. The low $R_s$ value indicates improved interfacial transport and favorable formation of the passivation layer. Furthermore, it was found that the charge transfer resistance of the electrolyte formulated with LiDFOB was lower as compared to the control electrolyte formulations. For the LiDFOB/$LiPF_4$ electrolyte, $LiPF_4$ electrolyte, and LiDFOB electrolyte, the reported charge-transfer resistance values were 81.7 Ω, 92.3 Ω, and 95.3 Ω, respectively. According to these findings, the combination of LiDFOB and $LiPF_4$ may lower charge-transfer resistance when compared to the separate electrolyte formulations, which might enhance electrochemical performance.

To accelerate the electrochemical performance of high energy density NMC bimodal/graphite full cells, the LiDFOB additive was incorporated into an electrolyte composed of EMC, EC, DEC and VC solvents. The addition of LiDFOB improved the cycling stability and rate performance. **Figures 7(a)-(f)** illustrate the surface morphology of pristine and cycled graphite electrodes in different electrolyte conditions. The pristine graphite revealed a characteristic multilayered struc-

ture (Figure 7(a), Figure 7(b)). The cycled electrodes revealed a bright surface layer, owing to the formation of the SEI. In the basic electrolyte with dissolved transition metal species, the graphite surface showed increased roughness and presence of large irregularly distributed luminescent agglomerates (Figure 7(c), Figure 7(d)), suggesting possible surface deposition of metal bearing species [43] [44]. Conversely, the graphite electrodes cycled in the electrolyte containing LiDFOB showed a much smoother and uniform surface morphology. This improvement can be attributed to the formation of a stable interfacial layer that prevents the transition metals from the cathode from dissolving and depositing on the graphite anode, thus facilitating the reversible intercalation/deintercalation of the lithium ions. In addition, the formation of a stable, ionically conductive interphase can promote Li+ transport at high current densities, resulting in an enhanced rate capability and cycling efficiency of the full cells.

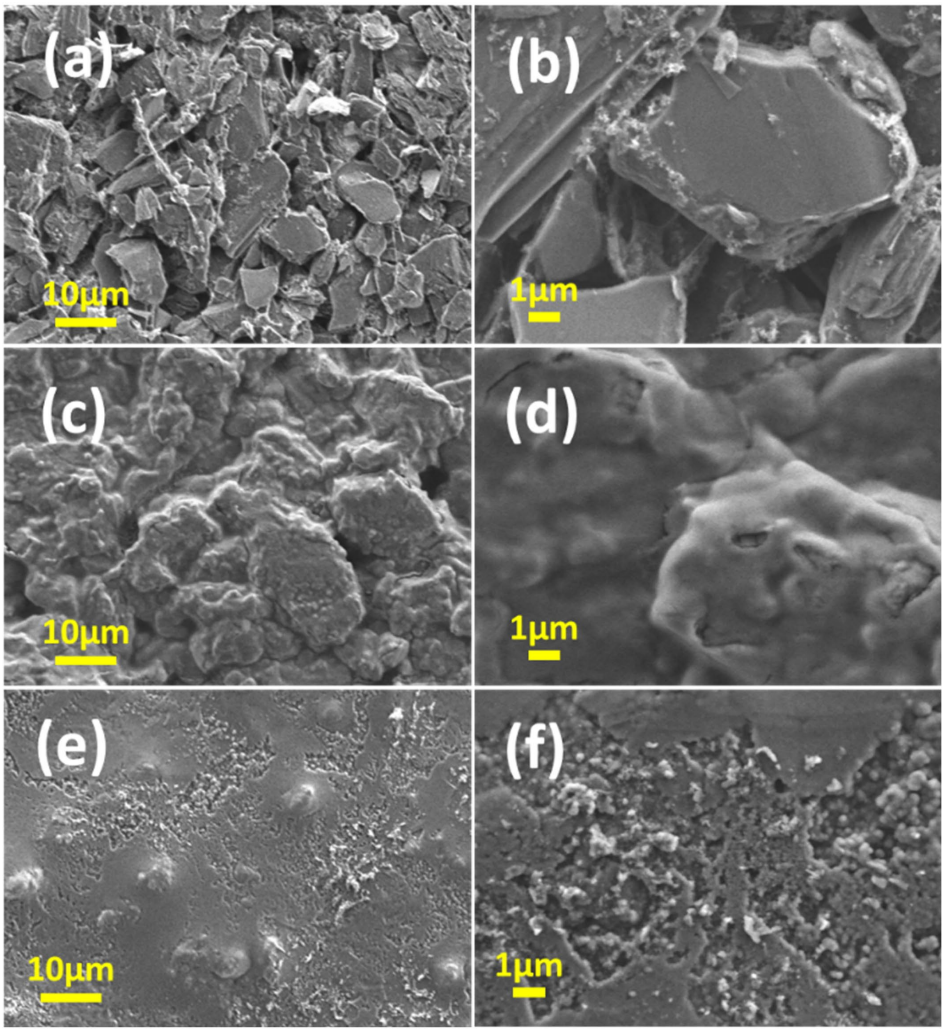



Figure 7. Representative the SEM images of the pristine and cycled graphite electrodes from NMC bimodel/Graphite full cell at room temperature. (a, b) Pristine electrode (c, d) Cycled electrodes were obtained from base electrolyte and (e, f) Cycled electrodes from 1 wt% LiDFOB electrolyte composition.

## 4. Conclusion

In this work, we developed different additive composition electrolytes applied for NMCbimodel/Li and NMCbimodel/Graphite cells. By optimizing the concentration of the additives, it has been found that by the addition of 1 wt% LiDFOB can improve the high capacity of 190 mAh/g with higher retention 85% compared then VC electrolyte capacity 120 mAh/g retention 60% and base electrolyte retention 10% after 90 cycles charge-discharge performance and explain the mechanism of LiDFOB-involved film formation. We conducted the electrochemical impedance spectroscopy (EIS) test on NMCbimodel/Li cell with different compositions base, VC, 1 wt% LiDFOB and 2 wt% LiDFOB, in this 1 wt% LiDFOB shows lower resistance than compared to other electrolyte compositions due to the LiDFOB additive forms the highly ionically conductive CEI and SEI layers formation. The 1 wt% LiDFOB additive as shown better retention compared to other composition, due to LiDFOB good compatibility anode and cathode, suppress the Mn ions dissolution from cathode material in NMCbimodel-Graphite cell.

## Data Availability Statement

The data that support the findings of this study are available inthe supplementary material of this article.

## Acknowledgements

The authors gratefully acknowledge Amara Raja Advanced Cell Technologies for providing the necessary support and granting permission to publish this work. Their continued encouragement and facilitation of research activities have been instrumental in the successful completion of this study.

## Author Contributions

Seggem Prabhakar: Writing-original draft, Conceptualization, Visualization, Methodology, Formal Analysis, Kirankumar R: Resources and review, Sethuraman V-Software and Data Curation, Satyanarayana M: Resources and review, Vasudeva rao P- Visualization and Investigation., Ebenezer D- Software and Data Curation, Aditya Ranjan Ray-Software and Data Curation.

## Conflicts of Interest

The authors declare no conflict of interest.

## References

[1] Xu, W., Wang, J., Ding, F., Chen, X., Nasybulin, E., Zhang, Y., *et al.* (2014) Lithium Metal Anodes for Rechargeable Batteries. *Energy Environ. Sci.*, **7**, 513-537. https://doi.org/10.1039/c3ee40795k

[2] Lin, D., Liu, Y. and Cui, Y. (2017) Reviving the Lithium Metal Anode for High-Energy Batteries. *Nature Nanotechnology*, **12**, 194-206. https://doi.org/10.1038/nnano.2017.16

[3] Pender, J.P., Jha, G., Youn, D.H., Ziegler, J.M., Andoni, I., Choi, E.J., *et al.* (2020) Electrode Degradation in Lithium-Ion Batteries. *ACS Nano*, **14**, 1243-1295. https://doi.org/10.1021/acsnano.9b04365

[4] Vetter, J., Novák, P., Wagner, M.R., Veit, C., Möller, K., Besenhard, J.O., *et al.* (2005) Ageing Mechanisms in Lithium-Ion Batteries. *Journal of Power Sources*, **147**, 269-281. https://doi.org/10.1016/j.jpowsour.2005.01.006

[5] Zhao, W., Ji, Y., Zhang, Z., Lin, M., Wu, Z., Zheng, X., *et al.* (2017) Recent Advances in the Research of Functional Electrolyte Additives for Lithium-Ion Batteries. *Current Opinion in Electrochemistry*, **6**, 84-91. https://doi.org/10.1016/j.coelec.2017.10.012

[6] Ren, X., Zhang, Y., Engelhard, M.H., Li, Q., Zhang, J. and Xu, W. (2017) Guided Lithium Metal Deposition and Improved Lithium Coulombic Efficiency through Synergistic Effects of $LiAsF_6$ and Cyclic Carbonate Additives. *ACS Energy Letters*, **3**, 14-19. https://doi.org/10.1021/acsenergylett.7b00982

[7] Beltrop, K., Klein, S., Nölle, R., Wilken, A., Lee, J.J., Köster, T.K., *et al.* (2018) Triphenylphosphine Oxide as Highly Effective Electrolyte Additive for Graphite/NMC811 Lithium Ion Cells. *Chemistry of Materials*, **30**, 2726-2741. https://doi.org/10.1021/acs.chemmater.8b00413

[8] Xia, Y., Zheng, J., Wang, C. and Gu, M. (2018) Designing Principle for Ni-Rich Cathode Materials with High Energy Density for Practical Applications. *Nano Energy*, **49**, 434-452. https://doi.org/10.1016/j.nanoen.2018.04.062

[9] Noh, H., Youn, S., Yoon, C.S. and Sun, Y. (2013) Comparison of the Structural and Electrochemical Properties of Layered $Li[Ni_xCo_yMn_z]O_2$ (X = 1/3, 0.5, 0.6, 0.7, 0.8 and 0.85) Cathode Material for Lithium-Ion Batteries. *Journal of Power Sources*, **233**, 121-130. https://doi.org/10.1016/j.jpowsour.2013.01.063

[10] Xu, K. (2004) Nonaqueous Liquid Electrolytes for Lithium-Based Rechargeable Batteries. *Chemical Reviews*, **104**, 4303-4418. https://doi.org/10.1021/cr030203g

[11] von Cresce, A. and Xu, K. (2011) Electrolyte Additive in Support of 5 V Li Ion Chemistry. *Journal of The Electrochemical Society*, **158**, A337. https://doi.org/10.1149/1.3532047

[12] Zhang, S.S. (2006) A Review on Electrolyte Additives for Lithium-Ion Batteries. *Journal of Power Sources*, **162**, 1379-1394. https://doi.org/10.1016/j.jpowsour.2006.07.074

[13] Aurbach, D., Gamolsky, K., Markovsky, B., Gofer, Y., Schmidt, M. and Heider, U. (2002) On the Use of Vinylene Carbonate (VC) as an Additive to Electrolyte Solutions for Li-Ion Batteries. *Electrochimica Acta*, **47**, 1423-1439. https://doi.org/10.1016/s0013-4686(01)00858-1

[14] Lee, H., Wang, Y., Wan, C., Yang, M., Wu, H. and Shieh, D. (2005) The Function of Vinylene Carbonate as a Thermal Additive to Electrolyte in Lithium Batteries. *Journal of Applied Electrochemistry*, **35**, 615-623. https://doi.org/10.1007/s10800-005-2700-x

[15] Burns, J.C., Petibon, R., Nelson, K.J., Sinha, N.N., Kassam, A., Way, B.M., *et al.* (2013) Studies of the Effect of Varying Vinylene Carbonate (VC) Content in Lithium Ion Cells on Cycling Performance and Cell Impedance. *Journal of The Electrochemical Society*, **160**, A1668-A1674. https://doi.org/10.1149/2.031310jes

[16] Xia, J., Aiken, C.P., Ma, L., Kim, G.Y., Burns, J.C., Chen, L.P., *et al.* (2014) Combinations of Ethylene Sulfite (ES) and Vinylene Carbonate (VC) as Electrolyte Additives in $Li(Ni_{1/3}Mn_{1/3}Co_{1/3})O_2$/Graphite Pouch Cells. *Journal of The Electrochemical Society*, **161**, A1149-A1157. https://doi.org/10.1149/2.108406jes

[17] Xu, Y., Liu, J., Zhou, L., Zeng, L. and Yang, Z. (2017) FEC as the Additive of 5 V Electrolyte and Its Electrochemical Performance for $LiNi_{0.5}Mn_{1.5}O_4$. *Journal of Electroanalytical Chemistry*, **791**, 109-116. https://doi.org/10.1016/j.jelechem.2017.03.017

[18] Yim, T. and Han, Y. (2017) Tris(trimethylsilyl) Phosphite as an Efficient Electrolyte Additive to Improve the Surface Stability of Graphite Anodes. *ACS Applied Materials & Interfaces*, **9**, 32851-32858. https://doi.org/10.1021/acsami.7b11309

[19] Liu, J., Song, X., Zhou, L., Wang, S., Song, W., Liu, W., *et al.* (2018) Fluorinated Phosphazene Derivative—A Promising Electrolyte Additive for High Voltage Lithium Ion Batteries: From Electrochemical Performance to Corrosion Mechanism. *Nano Energy*, **46**, 404-414. https://doi.org/10.1016/j.nanoen.2018.02.029

[20] Xu, M., Tsiouvaras, N., Garsuch, A., Gasteiger, H.A. and Lucht, B.L. (2014) Generation of Cathode Passivation Films via Oxidation of Lithium Bis(Oxalato) Borate on High Voltage Spinel ($LiNi_{0.5}Mn_{1.5}O_4$). *The Journal of Physical Chemistry C*, **118**, 7363-7368. https://doi.org/10.1021/jp501970j

[21] Mun, J., Lee, J., Hwang, T., Lee, J., Noh, H. and Choi, W. (2015) Lithium Difluoro(Oxalate)borate for Robust Passivation of $LiNi_{0.5}Mn_{1.5}O_4$ in Lithium-Ion Batteries. *Journal of Electroanalytical Chemistry*, **745**, 8-13. https://doi.org/10.1016/j.jelechem.2015.02.034

[22] Bian, X., Fu, Q., Bie, X., Yang, P., Qiu, H., Pang, Q., *et al.* (2015) Improved Electrochemical Performance and Thermal Stability of Li-Excess $Li_{1.18}Co_{0.15}Ni_{0.15}Mn_{0.52}O_2$ Cathode Material by $Li_3Po_4$ Surface Coating. *Electrochimica Acta*, **174**, 875-884. https://doi.org/10.1016/j.electacta.2015.06.085

[23] Zhu, Y., Luo, X., Xu, M., Zhang, L., Yu, L., Fan, W., *et al.* (2016) Failure Mechanism of Layered Lithium-Rich Oxide/Graphite Cell and Its Solution by Using Electrolyte Additive. *Journal of Power Sources*, **317**, 65-73. https://doi.org/10.1016/j.jpowsour.2016.03.090

[24] Wotango, A.S., Su, W., Leggesse, E.G., Haregewoin, A.M., Lin, M., Zegeye, T.A., *et al.* (2017) Improved Interfacial Properties of MCMB Electrode by 1-(Trimethylsilyl)Imidazole as New Electrolyte Additive to Suppress $LiPF_6$ Decomposition. *ACS Applied Materials & Interfaces*, **9**, 2410-2420. https://doi.org/10.1021/acsami.6b13105

[25] Aravindan, V., Gnanaraj, J., Madhavi, S. and Liu, H. (2011) Lithium-Ion Conducting Electrolyte Salts for Lithium Batteries. *Chemistry—A European Journal*, **17**, 14326-14346. https://doi.org/10.1002/chem.201101486

[26] Xu, M., Zhou, L., Hao, L., Xing, L., Li, W. and Lucht, B.L. (2011) Investigation and Application of Lithium Difluoro(Oxalate)borate (Lidfob) as Additive to Improve the Thermal Stability of Electrolyte for Lithium-Ion Batteries. *Journal of Power Sources*, **196**, 6794-6801. https://doi.org/10.1016/j.jpowsour.2010.10.050

[27] Xiao, A., Yang, L., Lucht, B.L., Kang, S. and Abraham, D.P. (2009) Examining the Solid Electrolyte Interphase on Binder-Free Graphite Electrodes. *Journal of The Electrochemical Society*, **156**, A318-A324. https://doi.org/10.1149/1.3078020

[28] Fu, M.H., Huang, K.L., Liu, S.Q., Liu, J.S. and Li, Y.K. (2010) Lithium Difluoro(Oxalato)Borate/Ethylene Carbonate+Propylene Carbonate+Ethyl(Methyl) Carbonate Electrolyte for $LiMn_2O_4$ Cathode. *Journal of Power Sources*, **195**, 862-866. https://doi.org/10.1016/j.jpowsour.2009.08.042

[29] Liu, M., Dai, F., Ma, Z., Ruthkosky, M. and Yang, L. (2014) Improved Electrolyte and Its Application in $LiNi_{1/3}Mn_{1/3}Co_{1/3}O_2$-Graphite Full Cells. *Journal of Power Sources*, **268**, 37-44. https://doi.org/10.1016/j.jpowsour.2014.05.109

[30] Wu, F., Zhu, Q., Chen, R., Chen, N., Chen, Y. and Li, L. (2015) Ionic Liquid Electrolytes with Protective Lithium Difluoro(Oxalate)borate for High Voltage Lithium-Ion Batteries. *Nano Energy*, **13**, 546-553. https://doi.org/10.1016/j.nanoen.2015.03.042

[31] Gao, H., Maglia, F., Lamp, P., Amine, K. and Chen, Z. (2017) Mechanistic Study of Electrolyte Additives to Stabilize High-Voltage Cathode-Electrolyte Interface in Lithium-Ion Batteries. *ACS Applied Materials & Interfaces*, **9**, 44542-44549. https://doi.org/10.1021/acsami.7b15395

[32] Zhang, L., Ma, Y., Cheng, X., Zuo, P., Cui, Y., Guan, T., *et al.* (2014) Enhancement of High Voltage Cycling Performance and Thermal Stability of $LiNi_{1/3}Mn_{1/3}Co_{1/3}O_2$ Cathode by Use of Boron-Based Additives. *Solid State Ionics*, **263**, 146-151. https://doi.org/10.1016/j.ssi.2014.06.001

[33] Delp, S.A., Borodin, O., Olguin, M., Eisner, C.G., Allen, J.L. and Jow, T.R. (2016) Importance of Reduction and Oxidation Stability of High Voltage Electrolytes and Additives. *Electrochimica Acta*, **209**, 498-510. https://doi.org/10.1016/j.electacta.2016.05.100

[34] Park, K., Yu, S., Lee, C. and Lee, H. (2015) Comparative Study on Lithium Borates as Corrosion Inhibitors of Aluminum Current Collector in Lithium Bis(Fluorosulfonyl)Imide Electrolytes. *Journal of Power Sources*, **296**, 197-203. https://doi.org/10.1016/j.jpowsour.2015.07.052

[35] Cha, J., Han, J., Hwang, J., Cho, J. and Choi, N. (2017) Mechanisms for Electrochemical Performance Enhancement by the Salt-Type Electrolyte Additive, Lithium Difluoro(Oxalato)Borate, in High-Voltage Lithium-Ion Batteries. *Journal of Power Sources*, **357**, 97-106. https://doi.org/10.1016/j.jpowsour.2017.04.094

[36] Qin, G., Zhang, J., Chen, H., Li, H., Hu, J., Chen, Q., *et al.* (2024) Lithium Difluoro(Oxalate)Borate as Electrolyte Additive to Form Uniform, Stable and LiF-Rich Solid Electrolyte Interphase for High Performance Lithium Ion Batteries. *Surfaces and Interfaces*, **48**, Article 104297. https://doi.org/10.1016/j.surfin.2024.104297

[37] Sun, M., Ji, J., Hu, M., Weng, M., Zhang, Y., Yu, H., *et al.* (2019) Overwhelming the Performance of Single Atoms with Atomic Clusters for Platinum-Catalyzed Hydrogen Evolution. *ACS Catalysis*, **9**, 8213-8223. https://doi.org/10.1021/acscatal.9b02305

[38] Zhu, Y., Li, Y., Bettge, M. and Abraham, D.P. (2012) Positive Electrode Passivation by Lidfob Electrolyte Additive in High-Capacity Lithium-Ion Cells. *Journal of The Electrochemical Society*, **159**, A2109-A2117. https://doi.org/10.1149/2.083212jes

[39] Dong, Q., Guo, F., Cheng, Z., Mao, Y., Huang, R., Li, F., *et al.* (2019) Insights into the Dual Role of Lithium Difluoro(Oxalato)Borate Additive in Improving the Electrochemical Performance of Nmc811||Graphite Cells. *ACS Applied Energy Materials*, **3**, 695-704. https://doi.org/10.1021/acsaem.9b01894

[40] Amine, K., Liu, J., Kang, S., Belharouak, I., Hyung, Y., Vissers, D., *et al.* (2004) Improved Lithium Manganese Oxide Spinel/Graphite Li-Ion Cells for High-Power Applications. *Journal of Power Sources*, **129**, 14-19. https://doi.org/10.1016/j.jpowsour.2003.11.007

[41] Zheng, Y., Xu, N., Chen, S., Liao, Y., Zhong, G., Zhang, Z., *et al.* (2020) Construction of a Stable $LiNi_{0.8}Co_{0.1}Mn_{0.1}O_2$ (NCM811) Cathode Interface by a Multifunctional Organosilicon Electrolyte Additive. *ACS Applied Energy Materials*, **3**, 2837-2845. https://doi.org/10.1021/acsaem.9b02486

[42] Ruess, R., Schweidler, S., Hemmelmann, H., Conforto, G., Bielefeld, A., Weber, D.A., *et al.* (2020) Influence of NCM Particle Cracking on Kinetics of Lithium-Ion Batteries with Liquid or Solid Electrolyte. *Journal of The Electrochemical Society*, **167**, Article 100532. https://doi.org/10.1149/1945-7111/ab9a2c

[43] Joshi, T., Eom, K., Yushin, G. and Fuller, T.F. (2014) Effects of Dissolved Transition Metals on the Electrochemical Performance and SEI Growth in Lithium-Ion Batteries. *Journal of The Electrochemical Society*, **161**, A1915-A1921. https://doi.org/10.1149/2.0861412jes

[44] Bhattacharya, S., Riahi, A.R. and Alpas, A.T. (2014) Thermal Cycling Induced Capacity Enhancement of Graphite Anodes in Lithium-Ion Cells. *Carbon*, **67**, 592-606. https://doi.org/10.1016/j.carbon.2013.10.032